American Journal of Electromagnetics and Applications
2013; 1(3): 44-52
Published online October 30, 2013 (http://www.sciencepublishinggroup.com/j/ajea)
doi: 10.11648/j.ajea.20130103.11

Electromagnetic scattering by approximately cloaked cylindrical bodies using homogeneous isotropic multi-layered materials

Hany M. Zamel[1, *], Essam El Diwany[1], Hadia El Hennawy[2]

[1]Electronics Research Institute – Microwave Engineering Dept.,Egypt
[2]Faculty of Engineering – Ain Shams University, Egypt

Email address:
res_ass@yahoo.com(H. M. Zamel)

To cite this article:
Hany M. Zamel, Essam El Diwany, Hadia El Hennawy. Electromagnetic Scattering by Approximately Cloaked Cylindrical Bodies Using Homogeneous Isotropic Multi-Layered Materials. *American Journal of Electromagnetics and Applications.* Vol. 1, No. 3, 2013, pp. 44-52.doi: 10.11648/j.ajea.20130103.11

Abstract: In cloaking, a body is hidden from detection by surrounding it by a coating consisting of an unusual anisotropic nonhomogeneous material. Its function is to deflect the rays that would have struck the object, guide them around the object, and return them to their original trajectory, thus no waves are scattered from the body. The permittivity and permeability of such a cloak are determined by the coordinate transformation of compressing a hidden body into a point or a line.Some components of the electrical parameters of the cloaking material(ε, μ) are required to have infinite or zero value at the boundary of the hidden object. Approximate cloaking can be achieved by transforming the cylindrical body (dielectric and conducting) virtually into a small cylinder rather than a line, which eliminates the zero or infinite values of the electrical parameters. The radially-dependent cylindrical cloaking shell can be approximately discretized into many homogeneous anisotropic layers; each anisotropic layer can be replaced by a pair of equivalent isotropic sub-layers, where the effective medium approximation is used to find the parameters of these two equivalent sub-layers. In this work, the scattering properties of cloaked cylindrical bodies (dielectric and conducting) are investigated using a combination of approximate cloaking, together with discretizing the cloaking material using pairs of homogeneous isotropic sub-layers. The solution is obtained by rigorously solving Maxwell equations using angular harmonics expansion. The scattering pattern, and the back scattering cross section against the frequency are studied for both transverse magnetic (TM_z) and transverse electric (TE_z) polarizations of the incident plane wave for different transformed body radii.

Keywords: Scattering by Cylindrical Bodies (Dielectric and Conducting), Cloaking by Layered Isotropic Materials, Approximate Cloaking

1. Introduction

Recently, the concept of electromagnetic cloaking has drawn considerable attention concerning theoretical, numerical and experimental aspects [1] - [8]. One approach to achieve electromagnetic cloaking is to deflect the rays that would have struck the object, guide them around the object, and return them to their original trajectory, thus no waves are scattered from the body [1]. In the coordinate transformation method for cloaking, the body to be hidden is transformed virtually into a point (3D or spherical configuration) or a line (2D or cylindrical configuration), and this transformation leads to radially nonhomogeneous profiles of anisotropic ε, μ in the cloaking coating. One problem for the line-transformed cloaks is that some components of the parameters (ε, μ) always have singularities at the inner boundary. For cylindrical cloak, ε_ϕ, μ_ϕ are infinite while ε_ρ, μ_ρ, ε_z, μ_z are zero. This requires the use of metamaterials which can produce such values, however, they are narrow band since they rely on using array of resonant elements (as split ring resonators) [9] - [12]. To avoid the problem of the infinite or zero material parameters at the hidden body boundary, two approaches are studied. The first is removing a thin layer from the inner boundary; however, cloaking is very sensitive to this removal [13]. Another technique to obtain approximate cloaking is to transform the hidden body virtually into a small object rather than a point or a line as shown in Fig. 1, which eliminates the zero or infinite values of the electrical parameters [14] – [16]. This, however, leads to some

scattering, since the hidden body is virtually transformed into a small object rather than a point or a line, and the scattering decreases as the transformed sphere radius is smaller.

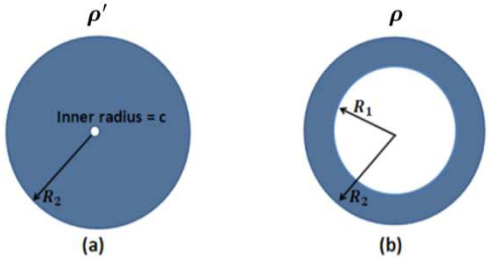

Fig. 1. *(a) Virtual domain, (b) Actual Domain*

The radially-dependent cylindrical cloaking shell can be approximately discretized into many homogeneous anisotropic layers, provided that the thickness of each layer is much less than the wavelength, and this discretization raises the level of scattering as the number of layers decreases. Each anisotropic layer can be replaced by a pair of equivalent homogeneous isotropic sub-layers A and B with different thicknesses, where the effective medium approximation is used to find the parameters of these two equivalent sub-layers [17]. The combination of approximate cloaking of a conducting cylinder with layered cloaking material is considered in [16].

In this work, the scattering properties of cloaked cylindrical bodies (dielectric and conducting) are investigated using a combination of approximate cloaking together with discretizing the cloaking material using pairs of homogeneous isotropic sub-layers. The solution is obtained by rigorously solving Maxwell equations using angular harmonics expansion. The scattering pattern, and the back scattering cross section against the frequency are studied for both TM_z and TE_z polarizations of the incident plane wave for different transformed body radii.

2. Coordinate Transformation Method for Cloaking - Material Parameters of the Approximate Cylindrical Cloak

Perfect cylindrical cloak can be constructed by compressing the electromagnetic fields in a cylindrical region $\rho' \le R_2$ into a cylindrical shell $R_1 \le \rho \le R_2$ as shown in Fig. 1. The coordinate transformation relates the radius ρ' in the virtual domain to the corresponding radius ρ in the cloaking material. The coordinate transformation is $\rho' = f(\rho)$, with $f(R_1) = 0$ for perfect cloaking or $f(R_1) = c$ for approximate cloaking and $f(R_2) = R_2$ [15], while φ and z are kept unchanged, where c is the reduced radius in the virtual domain. In the principal directions (ρ, φ, z in cylindrical coordinates) this transformation leads to a diagonal Jacobian matrix T [18], [19].

$$T = \begin{bmatrix} Q_\rho & 0 & 0 \\ 0 & Q_\varphi & 0 \\ 0 & 0 & Q_z \end{bmatrix} \tag{1}$$

whose elements are the stretching ratios (Q_ρ, Q_φ, Q_z) of the line elements in the principal directions $(\frac{d\rho'}{d\rho}, \frac{\rho' d\varphi'}{\rho d\varphi}, \frac{dz'}{dz}$ in cylindrical coordinates) in the virtual domain relative to the actual domain.

The radial and transverse permittivity and permeability of the cylindrical cloak, depending on ρ, are given as [1], [20]:

$$\frac{\varepsilon_\rho}{\varepsilon_0} = \frac{\mu_\rho}{\mu_0} = \frac{Q_\varphi Q_z}{Q_\rho} = \frac{f(\rho)}{\rho f'(\rho)}, \quad \frac{\varepsilon_\varphi}{\varepsilon_0} = \frac{\mu_\varphi}{\mu_0} = \frac{Q_\rho Q_z}{Q_\varphi} = \frac{\rho f'(\rho)}{f(\rho)}, \quad \frac{\varepsilon_z}{\varepsilon_0} = \frac{\mu_z}{\mu_0} = \frac{Q_\varphi Q_\rho}{Q_z} = \frac{f(\rho) f'(\rho)}{\rho} \tag{2}$$

A linear transformation is usually used, given for approximate cloaking by (for ideal cloaking c =0) [15], [21]:

$$f(\rho) = \rho' = \frac{1}{(R_2 - R_1)}[\rho(R_2 - c) + R_2(c - R_1)] \tag{3}$$

Thus, the permittivity and permeability of the approximate cylindrical cloak are given from the above equations by:

$$\frac{\varepsilon_\rho}{\varepsilon_0} = \frac{\mu_\rho}{\mu_0} = \frac{\rho(R_2 - c) + R_2(c - R_1)}{\rho(R_2 - c)} \tag{4}$$

$$\frac{\varepsilon_\varphi}{\varepsilon_0} = \frac{\mu_\varphi}{\mu_0} = \frac{\rho(R_2 - c)}{\rho(R_2 - c) + R_2(c - R_1)} \tag{5}$$

$$\frac{\varepsilon_z}{\varepsilon_0} = \frac{\mu_z}{\mu_0} = \frac{\rho(R_2 - c)^2 + R_2(c - R_1)(R_2 - c)}{\rho(R_2 - R_1)^2} \tag{6}$$

At $\rho = R_1$:

$$\frac{\varepsilon_\rho}{\varepsilon_0} = \frac{R_1(R_2 - c) + R_2(c - R_1)}{R_1(R_2 - c)} = \frac{c(R_2 - R_1)}{R_1(R_2 - c)} \tag{7}$$

$$\frac{\varepsilon_\varphi}{\varepsilon_0} = \frac{R_1(R_2 - c)}{R_1(R_2 - c) + R_2(c - R_1)} = \frac{R_1(R_2 - c)}{c(R_2 - R_1)} \tag{8}$$

$$\frac{\varepsilon_z}{\varepsilon_0} = \frac{R_1(R_2 - c)^2 + R_2(c - R_1)(R_2 - c)}{R_1(R_2 - R_1)^2} = \frac{c(R_2 - c)}{R_1(R_2 - R_1)} \tag{9}$$

For approximate cloaking ε_φ, μ_φ are proportional to $\frac{1}{c}$ at $\rho = R_1$, while ε_ρ, μ_ρ, ε_z, μ_z are proportional to c. Thus, for ideal cloaking (c=0), at the inner boundary, $\varepsilon_\varphi, \mu_\varphi$ are infinitely large, and the other components are zero.

At $\rho = R_2$:

$$\frac{\varepsilon_\rho}{\varepsilon_0} = \frac{R_2 - R_1}{R_2 - c} \tag{10}$$

$$\frac{\varepsilon_\varphi}{\varepsilon_0} = \frac{R_2 - c}{R_2 - R_1} \tag{11}$$

$$\frac{\varepsilon_z}{\varepsilon_0} = \frac{(R_2 - c)^2 + (c - R_1)(R_2 - c)}{(R_2 - R_1)^2} = \frac{R_2 - c}{R_2 - R_1} \tag{12}$$

The fields $E^i = [E^i_\rho, E^i_\varphi, E^i_z]$ and $H^i = [H^i_\rho, H^i_\varphi, H^i_z]$ in the virtual domain are related to the fields in the cloak medium $\hat{E}$, $\hat{H}$ by the relation $\hat{E} = T^t E^i$. For cylindrical cloaks [20]:

$$\hat{E}_\rho = f'(r)\, E^i_\rho(f(\rho),\varphi,z), \hat{H}_\rho = f'(\rho)\, H^i_\rho(f(\rho),\varphi,z) \quad (13)$$

$$\hat{E}_\varphi = \frac{f(\rho)}{\rho} E^i_\varphi(f(\rho),\varphi,z), \hat{H}_\varphi = \frac{f(\rho)}{\rho} H^i_\varphi(f(\rho),\varphi,z) \quad (14)$$

$$\hat{E}_z = E^i_z(f(\rho),\varphi,z),\ \hat{H}_z = H^i_z(f(\rho),\varphi,z) \quad (15)$$

3. Formulation of the Problem of Scattering by Cylindrical Layered Structure of Homogeneous Isotropic Materials

The radially-dependent cylindrical cloaking shell can be approximately discretized into many homogeneous anisotropic layers, provided that the thickness of each layer is much less than the wavelength, and this discretization raises the level of scattering as the number of layers decreases. Each anisotropic layer can be replaced by a pair of equivalent homogeneous isotropic sub-layers A and B with different thicknesses, where the effective medium approximation is used to find the parameters of these two equivalent sub-layers [17], as shown in Fig. 2.

To study scattering in cylindrical coordinates for normally incident field on the cylinder, Maxwell equations can be decomposed into TE_z (E_ρ, E_φ, H_z) and TM_z (H_ρ, H_φ, E_z) fields w.r.t the axial $\hat{z}$ direction. Thus, for TE_z fields only μ_z, ε_ρ and $\varepsilon_\varphi$are required when analyzing scattering. TM_z fields require $\varepsilon_z, \mu_\rho$and μ_φ.

3.1. The Parameters of the Isotropic Layers

When the layer thicknesses (d_A, d_B) are much less than the wavelength λ, the relationships between the anisotropic permittivities ε_ρ, ε_φ and the two- layer isotropic permittivities $\varepsilon_A, \varepsilon_B$ for TE_z polarization are given by [17]:

$$\varepsilon_\rho = \frac{(1+\eta)\varepsilon_A\varepsilon_B}{\varepsilon_B+\eta\varepsilon_A} \quad (16)$$

$$\varepsilon_\varphi = \frac{\varepsilon_A+\eta\varepsilon_B}{1+\eta} \quad (17)$$

In which, $\eta = d_B/d_A$,d_A and d_B are the thicknesses of layers A and B, respectively. These formulas correspond to series and parallel combinations of capacitors.

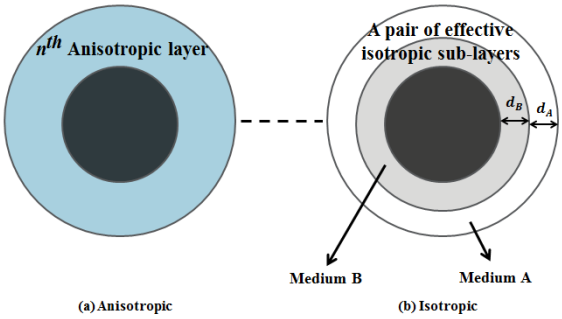

Fig.2. *Equivalence of an anisotropic cylindrical shell and two isotropic sub-shells*

By solving the above equations for $\varepsilon_A$and ε_B, one can obtain the equivalent medium parameters for the isotropic sub-layers when the thicknesses are identical ($\eta = 1$) :

$$\varepsilon_B = \varepsilon_\varphi + \sqrt{\varepsilon_\varphi{}^2 - \varepsilon_\varphi\varepsilon_\rho} \quad (18)$$

$$\varepsilon_A = \varepsilon_\varphi - \sqrt{\varepsilon_\varphi{}^2 - \varepsilon_\varphi\varepsilon_\rho} \quad (19)$$

which are used together with the axial permeability μ_z. Similar expressions hold for μ for TMz polarization. The values of ε_φ, $\varepsilon_\rho$and μ_z are taken at the average radius of the layer.

3.2. Scattering by a Cloaked Cylinder

The configuration for electromagnetic scattering by the cylindrical body (dielectric and conducting) coated by 2M layers is shown in Fig. 3. The external radius, permittivity, and permeability of the core and the layers are denoted by a_i, ε_i and μ_i(i= 1, 2, . . . , 2M+1), respectively. Fig. 3 shows an E_z polarized plane wave for TM_z case with amplitude E_0, $E^{inc} = E_o\, e^{-jk_0x}\hat{z}$, incident upon the coated cylinder along the $\hat{x}$ direction, where $k_0 = \omega\sqrt{\varepsilon_0\mu_0}$, $j = \sqrt{-1}$. The incident field can be expanded in angular harmonics for TE_z and TM_z cases as [22]:

$$E^{inc}_z = E_o \sum_{n=-\infty}^{\infty}(j)^{-n}J_n(k_0\rho)e^{jn\varphi} \quad (20)$$

$$H^{inc}_z = H_o \sum_{n=-\infty}^{\infty}(j)^{-n}J_n(k_0\rho)e^{jn\varphi} \quad (21)$$

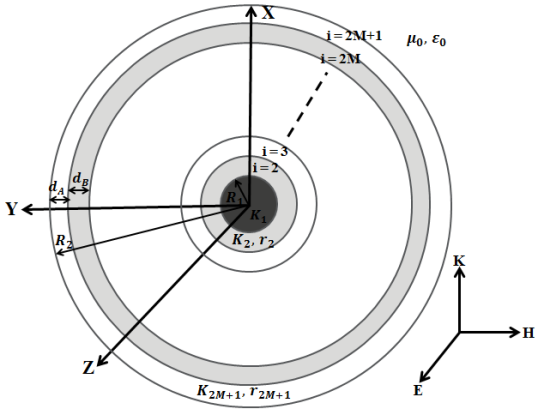

Fig.3. *Plane wave scattering by a multilayer dielectric cylinder*

WhereJ_n is the n^{th} order Bessel function of the first kind, n is integer. The time dependence of $e^{j\omega t}$ is suppressed.

The scattered E^s_z field for TMz polarization can be expanded as [22]:

$$E^s_z = E_o \sum_{n=-\infty}^{\infty}(j)^{-n}A_nH^2_n(k_0\rho)e^{jn\varphi} \quad (22)$$

Also, the scattered field H^s_z for TE_z polarization can be expanded as:

$$H^s_z = H_o \sum_{n=-\infty}^{\infty}(j)^{-n}B_nH^2_n(k_0\rho)e^{jn\varphi} \quad (23)$$

WhereH^2_n is the n^{th} order Hankel function of the second kind, $A_n$and B_n are coefficients to be determined.

For TM_z polarization, the field in the i^{th} layer can be expressed as:

$$E_z^i = E_o \sum_{n=-\infty}^{\infty}(j)^{-n}[C_n^i H_n^1(k_i\rho) + D_n^i H_n^2(k_i\rho)]\ e^{jn\varphi} \quad (24)$$

where $k_i = \omega\sqrt{\varepsilon_i\mu_i}$.
From Maxwell equation [22]:

$$H_\varphi^i = \frac{1}{j\mu\omega}\frac{\partial E_z^i}{\partial\rho} \quad (25)$$

Hence for TM_z polarization [22]:

$$H_\varphi^i = \frac{E_o}{j\eta_i}\sum_{n=-\infty}^{\infty}(j)^{-n}\begin{bmatrix} C_n^i[H_n^1(k_i\rho)]' \\ +D_n^i[H_n^2(k_i\rho)]' \end{bmatrix} e^{jn\varphi} \quad (26)$$

where $\eta_i = \sqrt{\frac{\mu_i}{\varepsilon_i}}$, and the prime over the square bracket indicates differentiation w.r.t. the argument.

For TE_z polarization, the field in the i^{th} layer can be expressed as:

$$H_z^i = H_o \sum_{n=-\infty}^{\infty}(j)^{-n}\begin{bmatrix} \tilde{C}_n^i H_n^1(k_i\rho) + \\ \tilde{D}_n^i H_n^2(k_i\rho) \end{bmatrix} e^{jn\varphi} \quad (27)$$

From Maxwell equation:

$$E_\varphi^i = \frac{-1}{j\omega\varepsilon}\frac{\partial H_z^i}{\partial\rho} \quad (28)$$

Hence,

$$E_\varphi^i = jH_o\eta_i \sum_{n=-\infty}^{\infty}(j)^{-n}\begin{bmatrix} \tilde{C}_n^i[H_n^1(k_i\rho)]' + \\ \tilde{D}_n^i[H_n^2(k_i\rho)]' \end{bmatrix} e^{jn\varphi} \quad (29)$$

For TM_z polarization, the boundary conditions are that the tangential components E_z and H_φ, respectively, are continuous across the cylindrical interfaces $\rho = a_i$ (i= 1, 2, . . . , 2M) and can be expressed as :

$$C_n^{i+1}H_n^1(k_{i+1}a_i) + D_n^{i+1}H_n^2(k_{i+1}a_i) = C_n^i H_n^1(k_i a_i) + D_n^i H_n^2(k_i a_i) \quad (30)$$

$$\sqrt{\frac{\epsilon_{i+1}}{\mu_{i+1}}}[C_n^{i+1}[H_n^1(k_{i+1}a_i)]' + D_n^{i+1}[H_n^2(k_{i+1}a_i)]'] = \sqrt{\frac{\epsilon_i}{\mu_i}}[C_n^i[H_n^1(k_i a_i)]' + D_n^i[H_n^2(k_i a_i)]'] \quad (31)$$

For TE_z polarization, the boundary conditions are that the tangential components H_z and E_φ , respectively, are continuous across the cylindrical interfaces $\rho = a_i$ $(i = 1, 2, \ldots, 2M)$ and can be expressed as :

$$\left[\tilde{C}_n^{i+1}H_n^1(k_{i+1}a_i) + \tilde{D}_n^{i+1}H_n^2(k_{i+1}a_i)\right] = \left[\tilde{C}_n^i H_n^1(k_i a_i) + \tilde{D}_n^i H_n^2(k_i a_i)\right] \quad (32)$$

$$\sqrt{\frac{\mu_{i+1}}{\epsilon_{i+1}}}\left[\tilde{C}_n^{i+1}[H_n^1(k_{i+1}a_i)]' + \tilde{D}_n^{i+1}[H_n^2(k_{i+1}a_i)]'\right] = \sqrt{\frac{\mu_i}{\epsilon_i}}\left[\tilde{C}_n^i[H_n^1(k_i a_i)]' + \tilde{D}_n^i[H_n^2(k_i a_i)]'\right] \quad (33)$$

The finiteness of the field in the dielectric core leads to the following ratios in the dielectric core [22]:

$$\frac{D_n^1}{C_n^1} = 1,\ \frac{\tilde{D}_n^1}{\tilde{C}_n^1} = 1 \quad (34)$$

When cloaking a conducting sphere, the dielectric constant in the core is taken to be very large.

The ratios D_n^{i+1}/C_n^{i+1} and $\tilde{D}_n^{i+1}/\tilde{C}_n^{i+1}$ in the successive larger layers can be obtained iteratively from the following equations [22]:

The ratios D_n^{i+1}/C_n^{i+1} and $\tilde{D}_n^{i+1}/\tilde{C}_n^{i+1}$ in the successive larger layers can be obtained iteratively from the following equations [22]:

$$\frac{D_n^{i+1}}{C_n^{i+1}} = -\frac{H_n^1(k_{i+1}a_i) - R_E^i H_n^{1\prime}(k_{i+1}a_i)}{H_n^2(k_{i+1}a_i) - R_E^i H_n^{2\prime}(k_{i+1}a_i)},\ i = 1,2,\ldots 2M \quad (35)$$

$$\frac{\tilde{D}_n^{i+1}}{\tilde{C}_n^{i+1}} = -\frac{H_n^1(k_{i+1}a_i) - R_H^i H_n^{1\prime}(k_{i+1}a_i)}{H_n^2(k_{i+1}a_i) - R_H^i H_n^{2\prime}(k_{i+1}a_i)},\ i = 1, \ldots.. 2M \quad (36)$$

where:

$$R_E^i = \sqrt{\frac{\mu_i\epsilon_{i+1}}{\epsilon_i\mu_{i+1}}}\frac{H_n^1(k_i a_i) + \frac{D_n^i}{C_n^i}H_n^2(k_i a_i)}{H_n^{1\prime}(k_i a_i) + \frac{D_n^i}{C_n^i}H_n^{2\prime}(k_i a_i)},\quad i = 1, 2, \ldots 2M \quad (37)$$

$$R_H^i = \sqrt{\frac{\mu_{i+1}\epsilon_i}{\epsilon_{i+1}\mu_i}}\frac{H_n^1(k_i a_i) + \frac{\tilde{D}_n^i}{\tilde{C}_n^i}H_n^2(k_i a_i)}{H_n^{1\prime}(k_i a_i) + \frac{\tilde{D}_n^i}{\tilde{C}_n^i}H_n^{2\prime}(k_i a_i)},\ i = 1, 2, \ldots 2M \quad (38)$$

Finally, the boundary conditions between the outer layer and air lead to the following equations:

$$J_n(k_0R_2) + A_nH_n^2(k_0R_2) = C_n^{2M+1}H_n^1(k_{2M+1}R_2) + D_n^{2M+1}H_n^2(k_{2M+1}R_2) \quad (39)$$

$$\sqrt{\frac{\epsilon_0}{\mu_0}}[[J_n(k_0R_2)]' + A_n[H_n^2(k_0R_2)]'] = \sqrt{\frac{\epsilon_{2M+1}}{\mu_{2M+1}}}\begin{bmatrix} C_n^{2M+1}[H_n^1(k_{2M+1}R_2)]' + \\ D_n^{2M+1}[H_n^2(k_{2M+1}R_2)]' \end{bmatrix} \quad (40)$$

$$J_n(k_0R_2) + B_nH_n^2(k_0R_2) = \tilde{C}_n^{2M+1}H_n^1(k_{2M+1}R_2) + \tilde{D}_n^{2M+1}H_n^2(k_{2M+1}R_2) \quad (41)$$

$$\sqrt{\frac{\mu_0}{\epsilon_0}}[[J_n(k_0R_2)]' + B_n[H_n^2(k_0R_2)]'] = \sqrt{\frac{\mu_{2M+1}}{\epsilon_{2M+1}}}\begin{bmatrix} \tilde{C}_n^{2M+1}[H_n^1(k_{2M+1}R_2)]' + \\ \tilde{D}_n^{2M+1}[H_n^2(k_{2M+1}R_2)]' \end{bmatrix} \quad (42)$$

From these equations, we can get the scattering coefficients A_n (TM_z case) and B_n (TE_z case):

$$A_n = -\frac{j_n(k_0R_2) - R_E^{2M+1}j_n'(k_0R_2)}{H_n^2(k_0R_2) - R_E^{2M+1}H_n^{2\prime}(k_0R_2)} \quad (43)$$

$$B_n = -\frac{j_n(k_0R_2) - R_H^{2M+1}j_n'(k_0R_2)}{H_n^2(k_0R_2) - R_H^{2M+1}H_n^{2\prime}(k_0R_2)} \quad (44)$$

The mode series is truncated at the mode number $n_{max} = k_0R_2 + 5$, [23].

3.3. The Scattering Width

For the 2-D scattering problem, the bistatic scattering width $\sigma(\varphi)$, which is referred to as the scattering cross section per unit length, is defined as [24]:

$$\sigma(\varphi) = \lim_{\rho\to\infty} 2\pi\rho \frac{|E^s(\varphi)|^2}{|E^i|^2} = \lim_{\rho\to\infty} 2\pi\rho \frac{|H^s(\varphi)|^2}{|H^i|^2} \quad (45)$$

The scattering width $\sigma(\varphi)$ defines the scattering in an arbitrary direction φ (for forward scattering $\varphi = 0^0$, for back scattering $\varphi = \pi$).

For TM_z case [24]:

$$\sigma(\varphi) = \frac{4}{k_0} |\sum_{n=0}^{\infty} (-1)^n \epsilon_n A_n \cos(n\varphi)|^2 \quad (46)$$

For TE_z case [24]:

$$\sigma(\varphi) = \frac{4}{k_0} |\sum_{n=0}^{\infty} (-1)^n \epsilon_n B_n \cos(n\varphi)|^2 \quad (47)$$

where the Neuman number

$$\epsilon_n = \begin{cases} 1 & \text{for } n = 0 \\ 2 & \text{for } n = 1,2,3,\ldots \end{cases}$$

4. Results

To check the above analysis, the far field scattering pattern for a conducting cylinder shelled with 2M layers of alternating dielectric layers A and B with identical thickness ($\eta = 1$) are calculated for M = 5 and 20, and compared with the results in [17], leading to identical results.

4.1. Conducting Cylinder

4.1.1. Normalized Bistatic Scattering Width

To show the effect of the cloaking radius c on the normalized bistatic scattering width, consider the inner cloaking core with radius $R_1 = \lambda$, the outermost radius $R_2 = 2R_1$, where λ is the wavelength, the cloak is discretized into 2M=40 layers.

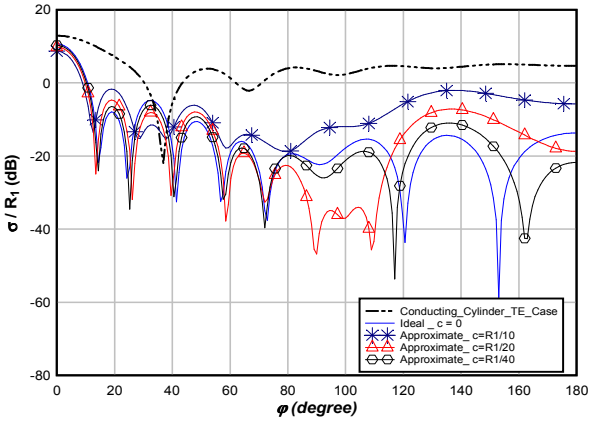

Fig.4. *Normalized bistatic scattering width for cloaked conducting cylinder with multilayered isotropic cloak for different reduced radii, TE_z case*

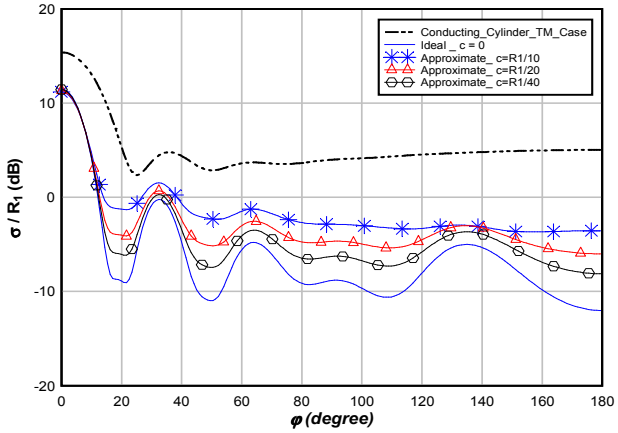

Fig. 5. *Normalized bistatic scattering width for cloaked conducting cylinder with multilayered isotropic cloak for different reduced radii, TM_z case*

Figures 4, 5 show the normalized bistatic scattering width (σ/R_1) versus the angle φ for cloaked conducting cylinder coated with multilayered isotropic homogenous layers for the ideal (c=0) and three different cloaking radii c for TE_z and TM_zcases, respectively. It can be seen from Figs. 4, 5 that, use of approximate cloaking ($c = R_1/10$, $R_1/20$and $R_1/40$) leads to reduction of the scattering compared with the uncoated conducting cylinder. The scattering from the layered cloak shows high endfire scattering ($\varphi = 0^0$), similar to the behavior of scattering from the uncloaked cylinder.

4.1.2. Normalized Back Scattering Width

Figures 6, 7 show the normalized back scattering width ($\sigma/\pi R_1$) versus the normalized frequency k_0R_1 for cloaked conducting cylinder coated with multi isotropic homogenous layers ($R_2 = 2R_1$, 2M = 40), for the ideal (c=0) and three different cloaking radii c for TE_z and TM_z cases, respectively. It can be seen from Figs. 6, 7, that when the reduced radius c decreases, the back scattering width decreases on the average. By setting $c = R_1/40$ the scattering approaches that of the ideal profile c =0. The back scattering width at low frequencies for TE_z case, Fig. 6, increases generally as the frequency increases, similar to the behavior of the scattering by the conducting cylinder, which results from the reflected and creeping waves. On the other hand, the back scattering width at low frequencies for TM_z case, Fig. 7, decreases generally as the frequency increases, similar to the behavior of the scattering by the conducting cylinder, which is high at low frequencies, since the incident electric field is parallel to the cylinder. The reduction of scattering by cloaking at low frequencies compared with the uncloaked conducting cylinder is more significant for TE_z polarization than for TM_z polarization.

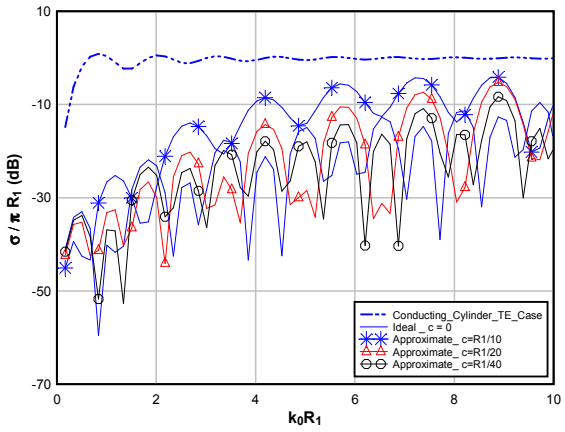

Fig. 6. Normalizedback scattering width of multilayered isotropic structure for different radii, TE$_z$ case

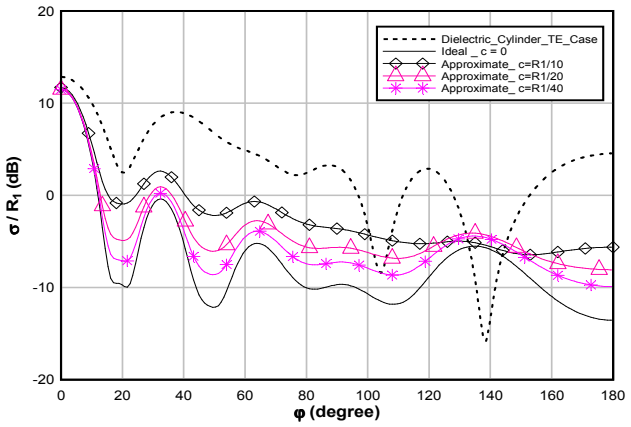

Fig. 8. Normalized bistatic scattering width for cloaked dielectric cylinder with $\varepsilon_d/\varepsilon_0 = 4$ for different radii, TE$_z$ case

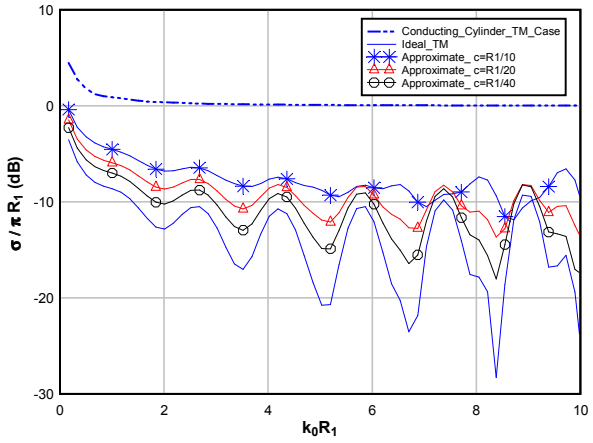

Fig. 7. Normalized back scattering width of multilayered isotropic structure for different radii, TM$_z$ case

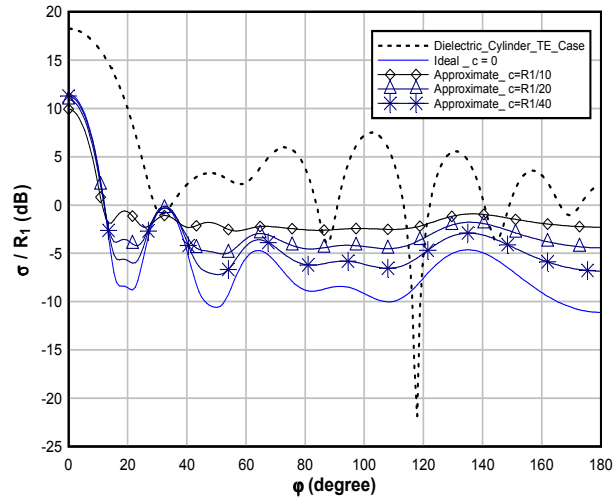

Fig. 9. Normalized bistatic scattering width for cloaked dielectric cylinder with $\varepsilon_d/\varepsilon_0 = 8$ for different radii, TE$_z$ case

4.2. Dielectric Cylinder

4.2.1. Normalized Bistatic Scattering Width

Figures 8, 9 show the normalized bistatic scattering width (σ/R_1) versus φ for cloaked dielectric cylinders with $\varepsilon_d/\varepsilon_0 = 4$ and 8, coated with multilayered isotropic homogenous layers for the ideal (c=0) and three different cloaking radii c for TE$_z$ case. At some angles the scattering with layered cloak is higher than that the dielectric cylinder, where the latter scattering has dips.The scattering from the layered cloak for $\varepsilon_d/\varepsilon_0 = 4$ and 8, shows high endfire scattering.

Figures 10, 11 show the normalized bistatic scattering width (σ/R_1) versus φ for cloaked dielectric cylinder with $\varepsilon_d/\varepsilon_0 = 4$ and 8,coated with multilayered isotropic homogenous layers for the ideal (c=0) and three different cloaking radii c for TM$_z$ case. The scattering pattern with cloaking for $\varepsilon_d/\varepsilon_0 = 4$ and 8 for TM$_z$ case is nearly identical to that for the conducting cylinder, Fig. 5, which means that the scattering is mainly produced by the cloak layers, not by the cloaked body.

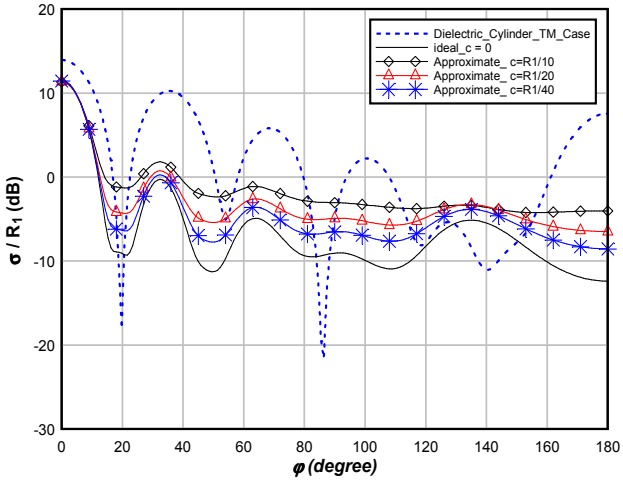

Fig. 10. Normalized bistatic scattering width for cloaked dielectric cylinder with $\varepsilon_d/\varepsilon_0 = 4$ for different radii, TM$_z$case

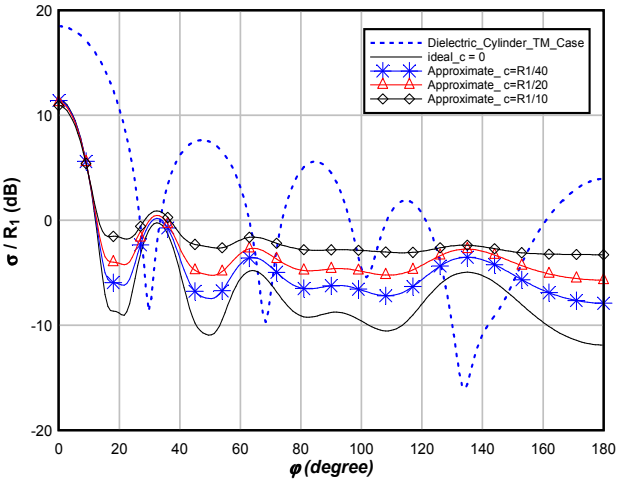

Fig. 11. *Normalized bistatic scattering width for cloaked dielectric cylinder with* $\varepsilon_d/\varepsilon_0 = 8$ *for different radii, TM$_z$ case*

4.2.2.Normalized Back Scattering Width

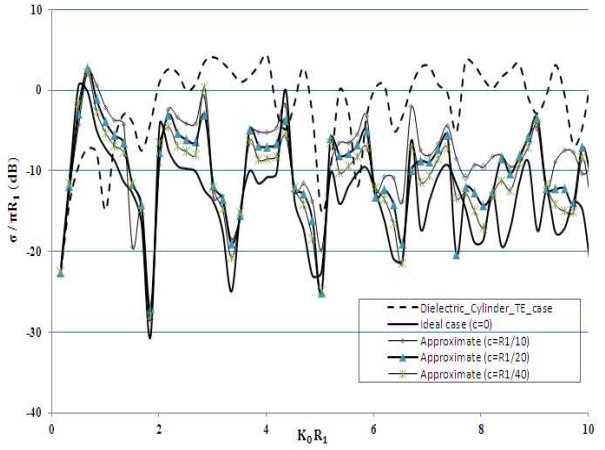

Fig. 12. *Normalized back scattering width for cloaked dielectric cylinder with* $\varepsilon_d/\varepsilon_0 = 4$ *for different radii, TE$_z$ case*

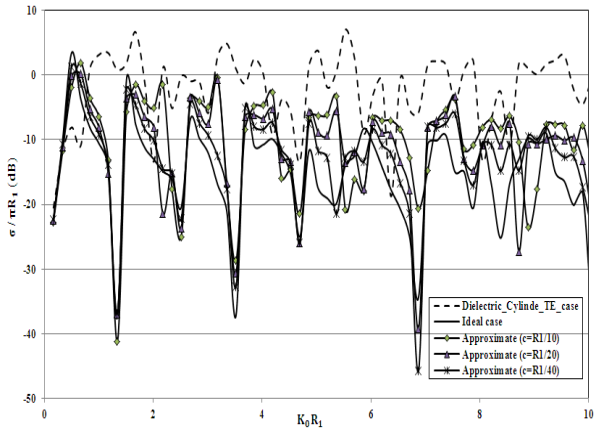

Fig. 13. *Normalized back scattering width for cloaked dielectric cylinder with* $\varepsilon_d/\varepsilon_0 = 8$ *for different radii, TE$_z$ case*

Figures 12, 13 show the normalized back scattering width ($\sigma/\pi R_1$) versus k_0R_1 of cloaked dielectric cylinder coated with multi isotropic homogeneous layers for the ideal (c=0) and three different cloaking radii c for TE$_z$ case, for $\varepsilon_d/\varepsilon_0 = 4$ and 8, respectively. At low frequencies, the scattering with layered cloak is higher than that from the dielectric cylinder. At the higher frequencies the normalized back scattering width decreases as the transformed radius c decreases. The behavior of the back scattering versus frequency shows resonance behavior, with the number of resonances increasing as ε_d increases.

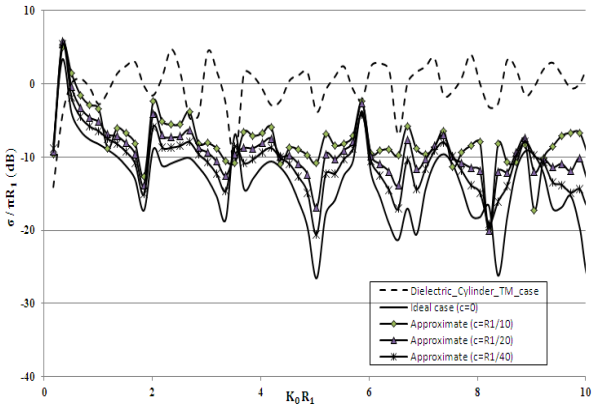

Fig. 14. *Normalized back scattering width for cloaked dielectric cylinder with* $\varepsilon_d = 4$ *for different radii, TM$_z$ case*

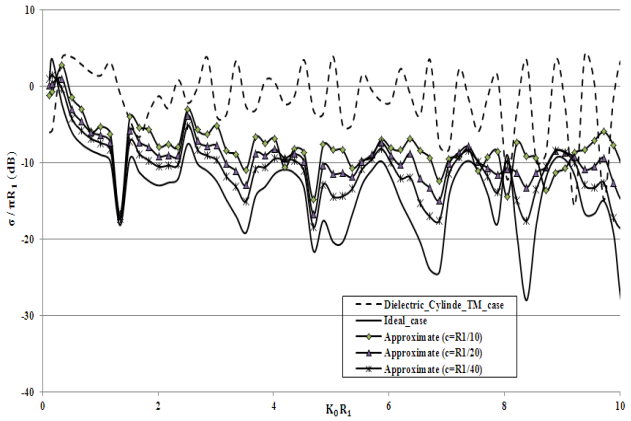

Fig. 15. *Normalized back scattering width for cloaked dielectric cylinder with* $\varepsilon_d/\varepsilon_0 = 8$ *for different radii, TM$_z$ case*

Figures 14, 15 show the normalized back scattering width versus k_0R_1 for cloaked dielectric cylinder coated with multilayered isotropic homogenous layers for the ideal (c=0) and three different cloaking radii c for TM$_z$ case, for $\varepsilon_d/\varepsilon_0 = 4$ and 8, respectively.

4.3. Permittivity and Permeability Profiles in the Cloak Layers

Figure 16 shows values of the material parameters in the cloaking layers for perfect cloaking c=0 and two different radii for approximate cloaks, Eqns. 4-6, 18, 19. We consider $R_2 = 2R_1$ and the cloak is discretized into 2M = 40 layers. For the ideal case, the value of the relative permittivity ε_φ at the inner boundary approaches infinity, Eqn. 8, but for approximate cloaking the value of $\varepsilon_B/\varepsilon_0$ at the inner layer is finite (53 for c=$R_1/20$ and 80 for c=$R_1/40$), Eqns. 7, 8,

18, as shown in Fig. 16. For ideal cloak (c = 0), μ_z is zero at the inner boundary, Eqn. 9, but for approximate cloaking the value of the relative permeability (μ_z/μ_0) is finite (0.18 for c=$R_1/20$ and 0.14 for c=$R_1/40$).

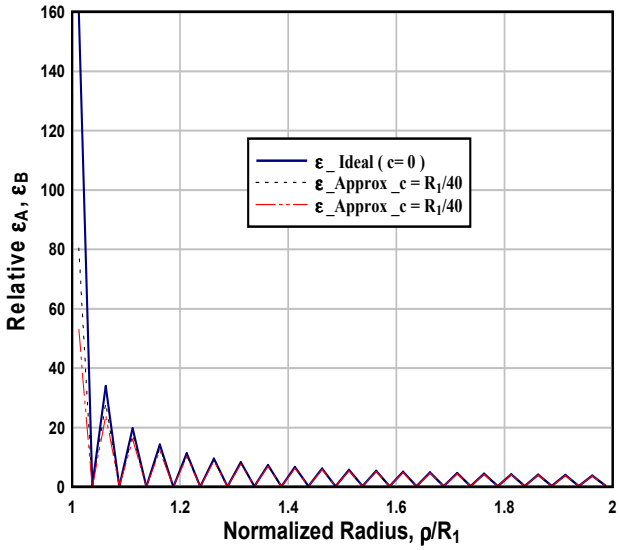

Fig. 16. *Relative permittivities$\varepsilon_{A,B}$ in the layers for the multilayered isotropic structure*

5. Conclusion

In this work, the scattering from approximately cloaked conducting and dielectric cylinders is studied for both TE_z and TM_z polarizations using multilayer cloak of isotropic homogenous layers. The anisotropic transverse components of ε (μ) for TE_z (TM_z) case are replaced by two isotropic layers, together with the single component of μ (ε). The solution is obtained iteratively for the angular modes amplitudes in the layers. The effect of approximate cloaking on removing the singular values of ε, μ components at the inner cloak radius shows that the components ε_φ, μ_φ vary as $\frac{R_1(R_2-c)}{c(R_2-R_1)}$, while the components ε_ρ, μ_ρ vary as $\frac{c(R_2-R_1)}{R_1(R_2-c)}$, and the components ε_z, μ_z vary as $\frac{c(R_2-c)}{R_1(R_2-R_1)}$. The scattering from the layered cloak shows high endfire scattering. The use of approximate cloaking leads to reduction of scattering compared with the uncoated conducting cylinder, particularly for TE_z polarization at low frequencies. The scattering from a cloaked dielectric cylinder at certain angles may be higher than the scattering from uncloaked cylinder at these angles where the scattering drops considerably. The back scattering versus frequency decreases on the average as the cloaking radius c decreases. The behavior of the back scattering versus frequency for cloaked dielectric cylinder shows resonance behavior, with the number of resonances increasing as ε_d increases. At high frequencies it decreases with decreasing c, whereas at low frequencies the reduction of scattering is much less, and even exceeds the scattering from uncloaked cylinder at a range of frequencies.

References

[1] J. B. Pendry, D. Schurig, and D. R. Smith, "Controlling electromagnetic fields," Science, Vol. 312, pp. 1780–1782, 2006.

[2] Q. Cheng, W. X. Jiang, and T. J. Cui, "Investigations of the electromagnetic properties of three-dimensional arbitrarily-shaped cloaks," Progress In Electromagnetics Research, Vol. 94, pp. 105 - 117, 2009.

[3] J. J. Yang, M. Huang, Y. L. Li, T. H. Li, and J. Sun, "Reciprocal invisible cloak with homogeneous metamaterials," Progress In Electromagnetics Research M, Vol. 21, pp. 105-115, 2011.

[4] A. Shahzad, F. Qasim, S. Ahmed, and Q. A. Naqvi, "Cylindrical invisibility cloak incorporating PEMC at perturbed void region," Progress In Electromagnetics Research M, Vol. 21, pp. 61-76, 2011.

[5] X. X. Cheng, H. S. Chen, and X. M. Zhang, "Cloaking a perfectly conducting sphere with rotationally uniaxial nihility media in monostatic radar system," Progress In Electromagnetics Research, Vol. 100, pp. 285-298, 2010.

[6] J. Zhang and N. A. Mortensen, "Ultrathin cylindrical cloak," Progress In Electromagnetics Research, Vol. 121, pp. 381-389, 2011.

[7] Y. B. Zhai and T. J. Cui, "Three-dimensional axisymmetric invisibility cloaks with arbitrary shapes in layered-medium background," Progress In Electromagnetics Research B, Vol. 27, pp. 151-163, 2011.

[8] D. Schurig, J. J. Mock, B. J. Justice, S. A. Cummer, J. B. Pendry, A. F. Starr, and D. R. Smith, "Metamaterial electromagnetic cloak at microwave frequencies," Science, Vol. 314, pp. 977-980, Oct. 2006.

[9] J. B. Pendry, A. J. Holden, D. J. Robbins, and W. J. Stewart, "Magnetism from conductors and enhanced nonlinear phenomena," IEEE Transactions on Microwave Theory and Techniques, Vol. 47, No. 11, pp. 2075 – 2084, Nov. 1999.

[10] G. V. Eleftheriades and K.G. Balmain, "Negative Refraction Metamaterials - Fundamental Principles and Applications," John Wiley, 2005.

[11] N. Engheta and R. W. Ziolkowski, "Metamaterials: Physics and Engineering Explorations," Wiley-IEEE Press, 2006.

[12] J. Wang, S. Qu, J. Zhang, H. Ma, Y. Yang, C. Gu, X. Wu, and Z. Xu, "A Tunable left-handed metamaterial based on modified broadside-coupled split-ring resonators," Progress In Electromagnetics Research Letters, Vol. 6, pp. 35-45, 2009.

[13] Z. Ruan, M. Yan, C. W. Neff, and M. Qiu, "Ideal cylindrical cloak: perfect but sensitive to tiny perturbations," Phys. Rev. Lett., Vol. 99, pp. 113903(1-4), 2007.

[14] H. Liu, "Virtual reshaping and invisibility in obstacle scattering," Inverse Problems, Vol. 25, No. 4, pp. 1-10, 2009.

[15] T. Zhou, "Electromagnetic Inverse Problems and Cloaking," Ph. D. Thesis, Washington University, 2010.

[16] W. Song, X. Yang and X. Sheng, "," IEEE Ant. and Propag.

Let. , Vol. 11, pp. 53- 56, 2012.

[17] Y. Huang, Y. Feng and T. Jiang, "Electromagnetic cloaking by layered structure of homogenous isotropic materials," Opt. Express, Vol. 15, No. 18, pp. 047602(1-4), 2007.

[18] J. McGuirk, "Electromagnetic Field Control and Optimization Using Metamaterials," Ph.D. Thesis, Air University, Ohio, U.S.A, 2009.

[19] J. Hu, X. Zhou and G. Hu, "Design method for electromagnetic cloak with arbitrary shapes based on Laplace's equation," Opt. Exp., Vol. 17, Iss. 15, pp. 13070-13070, 2009.

[20] M. Yan, W. Yan and M. Qiu, "Invisibility cloaking by coordinate transformation," Progress in Optics, Vol. 52, pp. 261-304, 2009.

[21] H. Zamel, E. El-Diwany and H. El-Hennawy, "Approximate electromagnetic cloaking of spherical bodies," 29^{th}National Radio Science Conference (NRSC), pp. 19-28, 2012, Egypt.

[22] J. Jin, "Theory and Computation of Electromagnetic Fields", John Wiley, 2010.

[23] C. Li and Z. Shen, "Electromagnetic scattering by a conducting cylinder coated with metamaterials," PIER, Vol. 42, pp. 91-105, 2003.

[24] G. T. Ruck, D. E. Barrick, W. D. Stuart and C.K. Krichbaum, "Radar Cross Section Handbook," Kluwer Academic, 1970.